Iraqi Journal of Physics, 2024
https://doi.org/10.30723/ijp.v22i3.1266

Vol. 22, No. 3, PP. 116-125
P-ISSN: 2070-4003
E-ISSN: 2664-5548

Physical Properties Studies of Magnesium Phthalocyanine (MgPc) Thin Films of Different Annealing Temperatures Prepared by Pulsed Laser Deposition Technique

Noora G. Adnan[1a*] and Eman K. Hassan[1b]
[1]*Department of Physics, College of Science, University of Baghdad, Baghdad, Iraq*
[b]Email: eman.hasan@sc.uobaghdad.edu.iq
[a*] Corresponding author: nora.Ghassan1604a@sc.uobaghdad.edu.iq

Abstract

Magnesium Phthalocyanine (MgPc) was deposited on a glass substrate by pulsed laser deposition (PLD) using Q-Switching Nd:YAG laser with wavelength 1064 nm, repetition rate 6 Hz, at room temperature (300K) and different annealing temperatures (373, 473, and 573) K under vacuum condition of 10^{-3} torr. All films were annealed for one hour to attain crystallinity. X-ray diffraction (XRD) of MgPc powder indicated that MgPc crystallizes in polycrystalline with a monoclinic structure. While comparing the MgPc films, it was observed that the intensity of the characteristic peak increases with temperature, and the crystallization exhibited a monoclinic structure typical of the β-form. The Miller indices, hkl, values for each diffraction peak in the XRD spectrum were calculated. The characteristic peak of Phthalocyanine (MgPc) was found at 2θ value 6.9137° with the hkl value of (100) for both MgPc powder and deposited thin films. Field emission scanning electron microscopy (FE-SEM), energy-dispersive X-ray spectroscopy (EDX) analyses, and atomic force microscopic (AFM) indicated that crystallinity improved and surface morphology was enhanced with the rise in annealing temperature and showed uniform-sized grains. They also assisted in identifying the optimal parameters that yielded the best structural properties for the thin film. The optical properties of MgPc thin film showed two absorption bands. The MgPc thin films exhibit transport and onset direct energy gaps (E_g) for all samples. Additionally, the absorption coefficient (α) was calculated using Lambert Law, revealing a slight dependence on the annealing temperature. FT-IR) spectra for (MgPc) and (H_2Pc) were determined.

Article Info.

Keywords:
Organic MgPc, PLD Technique, FE-SEM, AFM, Energy Gap.

Article history:
Received: Mar. 19, 2024
Revised: Jun. 25, 2024
Accepted: Jul. 08, 2024
Published:Sep.01, 2024

1. Introduction

Natural semiconductors are garnering considerable attention due to heightened activity in their synthesis and potential applications in a range of large-area flexible, disposable photonic, electronic, and electric devices, including sensors, organic light-emitting diodes (OLEDs), solar cells, memory devices, organic field-effect transistors [1, 2], junction diodes, and rechargeable batteries [3-9]. Phthalocyanines are a class of organic semiconductors known for their thermal and chemical stability; commercially recognized as blue-green pigments due to their strong absorption in the UV-Vis spectral region [10, 11]. Eley [12] was the first one to recognize the semiconducting characteristics of Phthalocyanines. Non-metallic phthalocyanines contain two hydrogen molecules in the atom's core. To increase the flexibility of electrons, two hydrogen molecules have been substituted with a single metal molecule, Mg, as illustrated in Fig. 1.

Magnesium phthalocyanine (MgPc) is a P-type semiconductor with a band gap of 2.6 eV [13]. It is characterized by significant thermal and chemical stability. MgPc has been utilized in various industrial applications, including optical communication storage, gas sensors, photovoltaic cells, liquid crystals, solar cells, and semiconducting apparatus [14]. It is challenging to manufacture phthalocyanine compounds utilizing

solution casting procedures since most of these elements are insoluble in the organic solvents often utilized [15-17]. Pulsed Laser Deposition (PLD) is frequently used to produce phthalocyanine thin films. This technique has the benefit of making films of high purity, and also makes it possible to cultivate somewhat complicated materials [18-21]. MgPc has the potential to manifest several polymorphic phases, namely α, β, and χ, which are associated with distinct crystalline structures. The metastable α and the stable β forms are the most often utilized. In the crystal structure, the slope molecule angle inside the columns and the grouping of the common columns are the primary factors that differentiate the two forms (the similarities and differences). Variations in conductivity across stacking molecules are significantly influenced by these characteristics, which have a substantial effect.

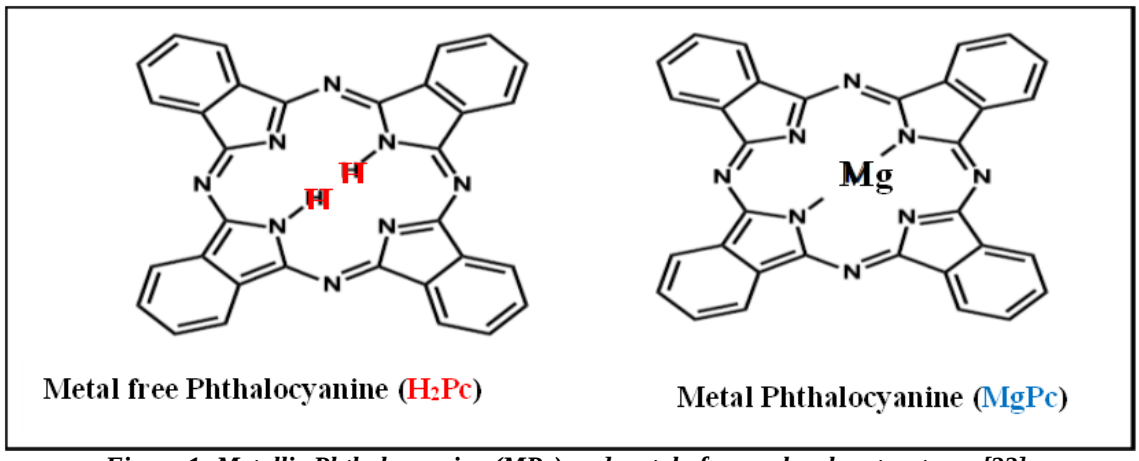

Figure 1: Metallic Phthalocyanine (MPc) and metals-free molecular structures [22].

The primary objective of this research was to obtain information on the molecular orientation, the distribution of polymorphic phase, and the grain size of MgPc. The PLD was utilized to deposit a thin coating of MgPc on a glass substrate to determine changes that occur as a consequence of the shoot pulses process [23-25].

2. Experimental Work

The PLD method was employed to sublime pure MgPc powder obtained from Luminescence Technology Corp. The powder was sublimed under a vacuum of 10^{-3} torr. To create a homogeneous target, 0.5 g of MgPc was crushed under 6 tons was employed as a material source for the PLD process. Thin films of MgPc were deposited on glass substrates, which were carefully cleaned with filtered water and ultrasonically agitated under acetone. For deposition, a Nd:YAG Q-Switching laser beam with a laser energy of 300 mJ, a wavelength of 1064 nm, and pulsed width with a repetition frequency of 6 Hz was utilized. The deposited films were annealed at different annealing temperatures (373, 473, and 573) K for one hour to attain crystallinity. An investigation into the elemental analysis of MgPc films was conducted using energy-dispersive X-ray spectroscopy (EDX) with an X-ray spectrometer (Bruker Nano GmbH, Germany). The crystal structure of MgPc was identified with an X-ray diffractometer (SHIMADZU XRD-6000, made in Japan) with Cuk_{α} radiation of 15406nm. The Field emission scanning electron microscope (FE-SEM) (TESCAN $MIRA_3$, made in the Czech Republic) was used to investigate the surface morphology and cross-section structure of MgPc films. Atomic Force Microscopy (AFM) (CSPM-AA3000, made in USA) was used to study the surface morphology and the dimensions of the surface grain size. A laser interferometer was utilized to determine the thickness of the films. This measurement was done in the electro-optics Laboratory, Department of Physics. A Fourier transform infrared spectrometer (SHIMADZU- IRPrestige-21) was used to obtain the infrared spectra at

normal temp and a frequency of 6Hz. A UV-visible Spectrophotometer (SHIMADZU-UV-1800) was used to record the ultraviolet and visible spectra. This instrument was also utilized to measure the transmittance and absorbance spectra in the range of 200-1100 nm for the thin films produced using MgPc.

3. Results and Discussion

3.1. Field Emission Scanning Electron Microscope Analyses (FE-SEM)

3D FE-SEM images were used to analyse the deposited films' structural surface. Fig. 2(a) displays the surface morphology of the films deposited at room temperature, which appear non-uniform with small particles and a coarse micro structure. Changes in the morphology and size of the deposited film particles were noted due to the variation in the annealing temperature. Increasing the annealing temperature resulted in a film with more uniformly sized particles compared to those produced at lower temperatures, as shown in Fig. 2 (b, c, and d). Furthermore, the increase in temperature has caused significant surface changes. The grain size (D) calculated from FE-SEM images varied from 32.605 to 37.514 nm.

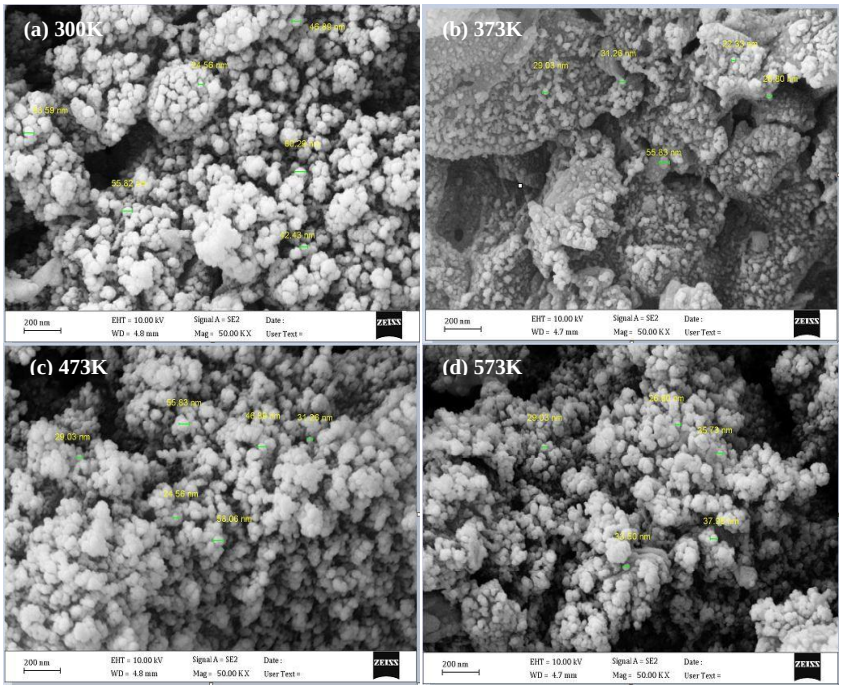

Figure 2: FE-SEM images of MgPc thin films at different annealing temperatures (a) 300K, (b) 373K, (c) 473K, and (d) 573K.

3.2. Energy Dispersive X-ray (EDX) Analysis

The EDX pattern of MgPc thin film is shown in Fig. 3. It demonstrates the existence of magnesium, nitrogen, hydrogen, and carbon by creating the C: H: N: Mg pattern. A strong peak of carbon was detected in the spectrum due to the chemical stoichiometry composition, which was ($C_{32}H_{16}N_8Mg$). The relative atomic weight, Table 1, shows that the highest weight percentage was carbon.

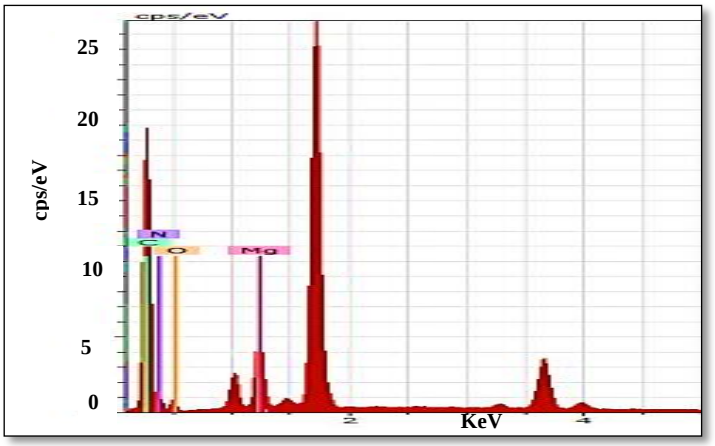

Figure 3: Energy Dispersive X-ray Spectroscopy (EDX) of MgPc thin film.

Table 1: The relative atomic weight percentage for MgPc.

Element	The relative atomic weight (%)
Carbon	70.31
Nitrogen	19.83
Oxygen	7.21
Magnesium	2.65

3.3. X-ray Diffraction (XRD) Analysis

Fig. 4 shows the XRD pattern of pure magnesium phthalocyanine powder at 300 K. The sequence of crystalline peaks is a result of the polycrystalline structure of MgPc. The Phthalocyanine peak appears at a 2θ of 6.9137°, corresponding to an hkl value of (100).This aligns well with the results of El-Nahass et al. [26].

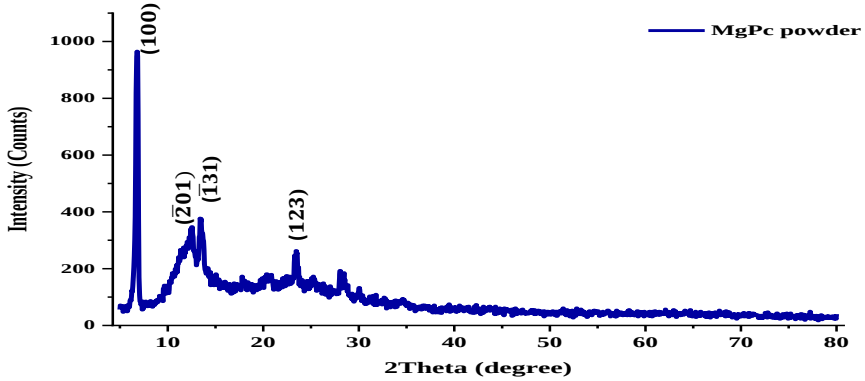

Figure 4: X-ray diffraction analysis of magnesium phthalocyanine powder.

Fig. 5 shows the XRD patterns of the MgPc thin films at room temperature of 300K and different annealing temperatures of 373K, 473K, and 573K. The XRD patterns of the MgPc thin films showed that the intensity of the peak increased as the annealing temperature was increased. The patterns revealed a monoclinic crystalline in the β-form.

The mean crystallite (D) size of the films was determined utilizing the Scherer formula [27-29]:

$$D = \frac{K s \lambda}{\beta` \cos\theta} \qquad (1)$$

where: λ is the X-ray wavelength of Cuk$_\alpha$ (0.15418 nm), Ks refers to a Scherer constant of the order of unity (≈0.95), $\beta` = \sqrt{\beta^2 f - \beta^2 p}$ (where β_f refers to the (100) peak full width at half maximum for the thin film, and β_p refers to the (100) peak full width at half maximum for the powder) operating in the same instrumental situations, θ is the corresponding Bragg angle. Table 2 lists the crystallite sizes of the MgPc deposited thin films for the different annealing temperatures. It can be noted that the crystallite size increased with the increase of the peak width as a result of increasing the thin films annealing temperature. The best annealing temperature was found to be 473K, which indicates the crystallization of the thin film in the β-form. The noted crystallite size decreased at 573K due to the rearrangement of atoms in the molecule.

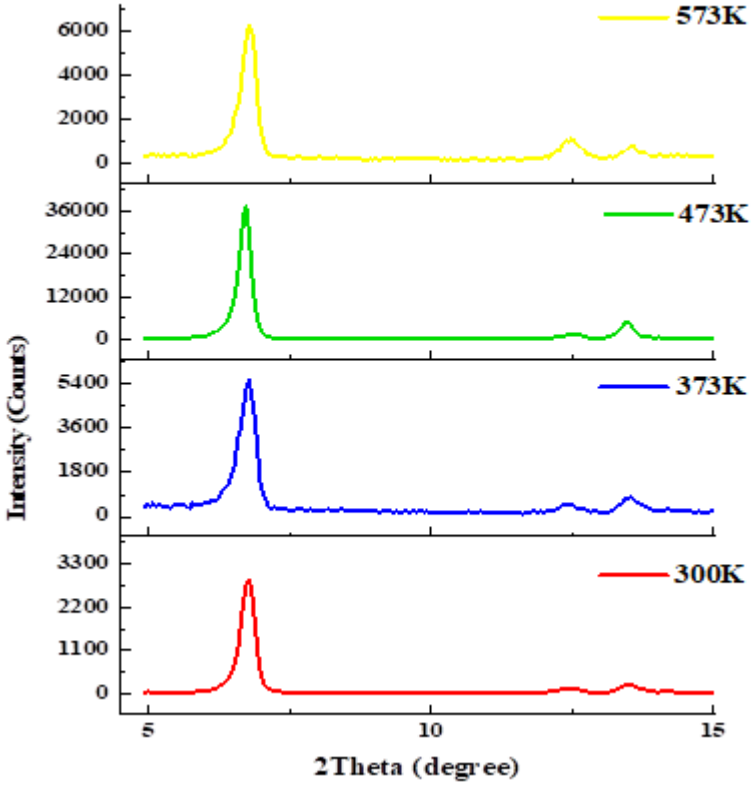

Figure 5: XRD of MgPc thin films at 300K room temperature and different annealing temperatures of (373, 473, and 573) K.

Table 2: The crystallite size (D) in the β-form of the MgPc deposited thin films at various annealing temperatures (300, 373, 473, 573) K.

Annealing temp.(K)	2Theta (deg.)	β_f (degree)	D (nm)
300	6.775	0.31343	21.12
373	6.775	0.28107	24.66
473	6.775	0.39316	29.54
573	6.775	0.33676	26.49

3.4. Atomic Force Microscope (AFM)

The deposited MgPc film morphology at various annealing temperatures of (300, 373, 473, and 573) K was analysed with an atomic force microscope (AFM), as illustrated in Fig. 6. It is demonstrated that, with increased annealing temperature, the film's structure became uniformly distributed with needle-like characteristics, and the

size of the grains decreased. This suggests that the grain growth occurring enhanced the crystallinity and improved the surface morphology [30]. The surface roughness and size of the grains are displayed in Table 3.

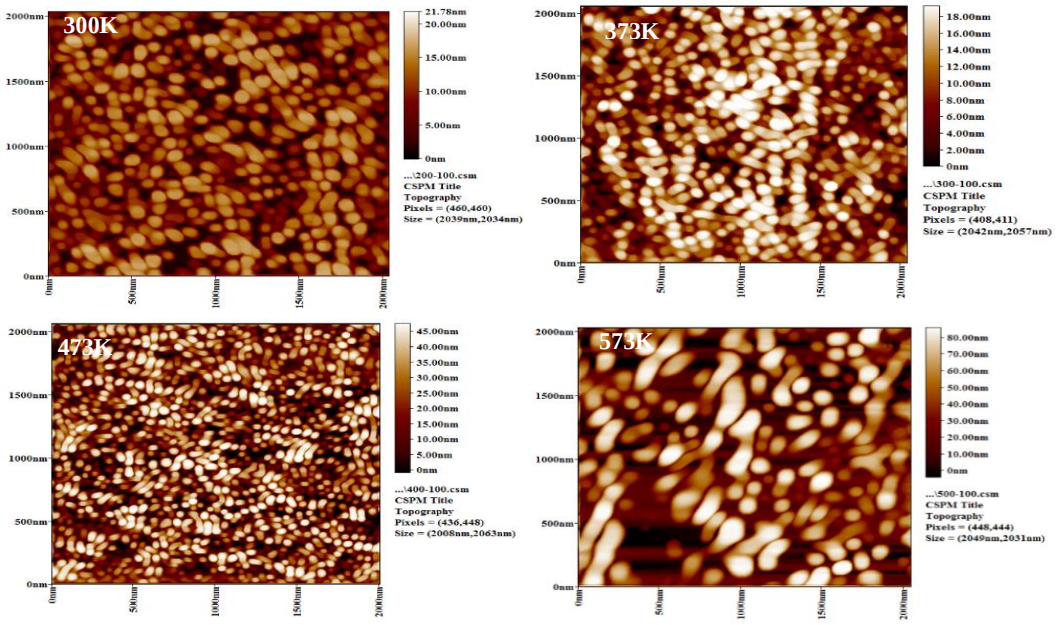

Figure 6: AFM images of MgPc thin films at different annealing temperatures (300,373,473,573) K.

Table 3: The surface roughness and grain size magnitudes of MgPc thin films at various annealing temperatures (300,373,473,573) K.

Annealing temp (K)	Roughness Mean (nm)	Root mean square (nm)	Avg. Diameter (nm)
300	382×10^{-2}	450×10^{-2}	7251×10^{-2}
373	448×10^{-2}	524×10^{-2}	6078×10^{-2}
473	1210×10^{-2}	1400×10^{-2}	6256×10^{-2}
573	2250×10^{-2}	2600×10^{-2}	8710×10^{-2}

3.5. Optical Analyses

Optical measurements are crucial to identify the band structure of semiconductors. The optical constants of thin films offer insights into the material's microscopic features, which are essential for applications in devices. Optical absorbance spectra were recorded over a wavelength range of 200-1100 nm using a UV-Vis spectrophotometer. The resulting data was utilized to calculate the absorption coefficient (α) based on the relationship between the intensity of incident light. (I_o) and the transmitted intensity (I_T) is represented by an exponential form Lambert Law [31]:

$$I_T = I_o \exp(-\alpha t) \qquad (2)$$

where α being the absorption coefficient and t is the film thickness. According to this Eq. (2), the optical absorption coefficient of thin films was evaluated from the transmittance data using the relation:

$$\alpha = 2.303 \frac{A}{T} \qquad (3)$$

where $T=I_T/I_o$ is defined as the transmittance [31]. As a result of absorption coefficient data, and the band gap energy (E_g) is determined. According to Tauc relation [32] given by:

$$\alpha h\upsilon = B\,(E - E_g)^{1/2} \qquad (4)$$

Fig. 7 illustrates the absorbance spectra of the UV-Vis region for the deposited MgPc thin films at different annealing temperatures across a range of wavelengths of (200-1100) nm. The spectra demonstrate two bands. One band, known as the B-band (or Soret) appears in the UV zone, resulting from a direct transition between the bonding π in HOMO and the antibonding π* in LUMO for all the specimens. The second band, known as the Q-band, is observed in the visible region and consists of two closely spaced peaks that indicate splitting characteristics (Davydov splitting). Table (4) provides the further details on the peaks of both bands. In their work, Santanu et al. [33-35] discussed the Q-band and Soret band of phthalocyanines, comparing them with other metals.

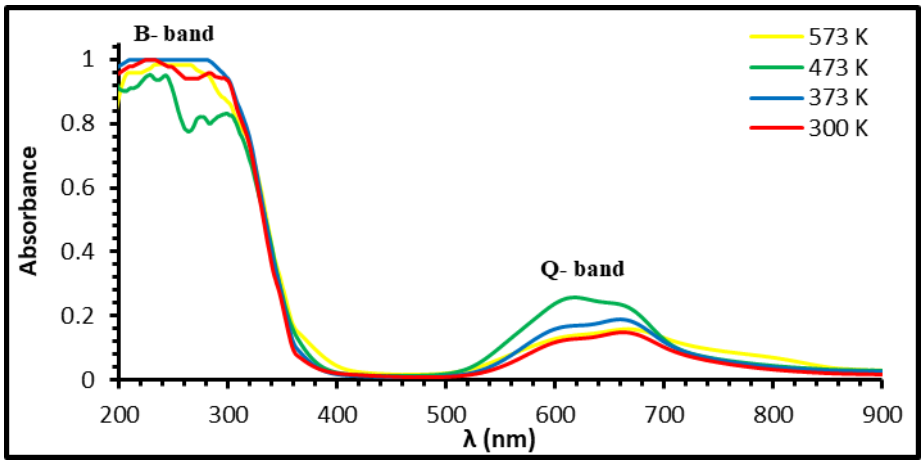

Figure 7: Absorbance spectra of MgPc thin films at different annealing temperatures.

Table 4: The magnitudes of the B and Q bands for MgPc at various annealing temperatures (300, 373, 473, 573) K

Annealing temp.(K)	B-band(nm)	Q-band(nm)
300	210-250	600-680
373	210-270	600-660
473	220-250	600-670
573	220-270	600-670

Figs. 8(a, b) display the optical band gaps for the Q- and B-band edge, which were determined by extending the straight line of $(\alpha h\nu)^2$ against hν graphical representations to $(\alpha h\nu)^2 = 0$ to obtain the energy band gaps of the MgPc deposited thin films at various annealing temperatues (300, 373, 473, 573) K. Table 5 displays the bandgaps of the Q and B in MgPc thin films.

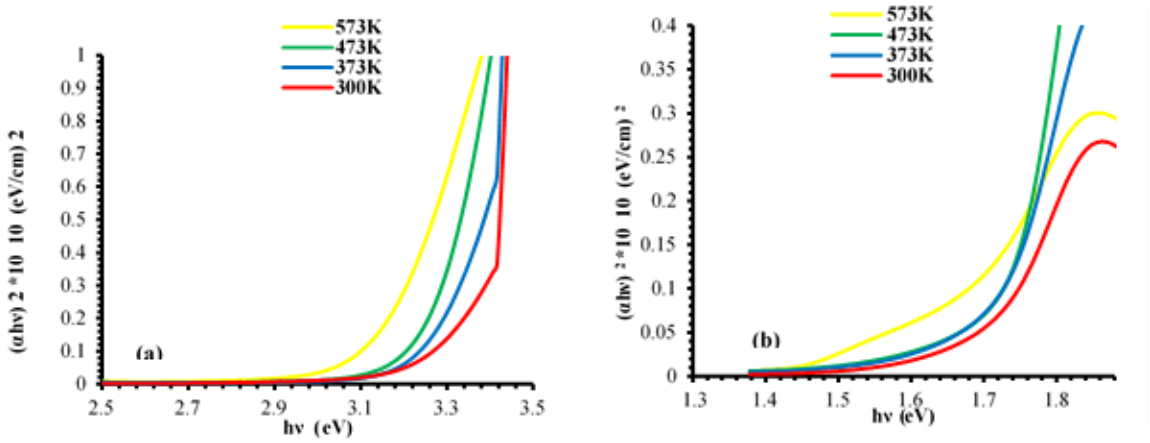

Figure 8: The band gap energy of the MgPc thin films at various annealing temperatures (300, 373, 473, 573) K for a) B-band and b) Q-band.

Table 5: The band gap energy for the Q and B bands of MgPc thin films at different annealing temperatures.

Annealing temp.(K)	Band gap energy (eV) B-band	Band gap energy (eV) Q-band
300	3.28	1.68
373	3.24	1.7
473	3.22	1.71
573	3.125	1.62

The Fourier Transform Infrared (FT-IR) spectra for MgPc Powder and Phthalocyanine metal free (H_2Pc) were determined at 300K, as illustrated in Fig. 9. The FT-IR spectrum illustrates the bond bending within the range of 400-2000 cm^{-1} and bond stretching within the range of 2000-4000 cm^{-1}. Based on Fig. 9, it is evident that the bond vibrating at 725.23 cm^{-1} was designated for (magnesium-nitrogen). The peak at 1280.73-1165.00 cm^{-1} indicates the stretching bond of C-N. Other bands include the C-H band at 1477.47 cm^{-1} and the N-H band at 3421 cm^{-1}. Furthermore, the bands at 1330.88 cm^{-1} and 1076.28 cm^{-1} are associated with C-C and C-H, as shown in the figure [36].

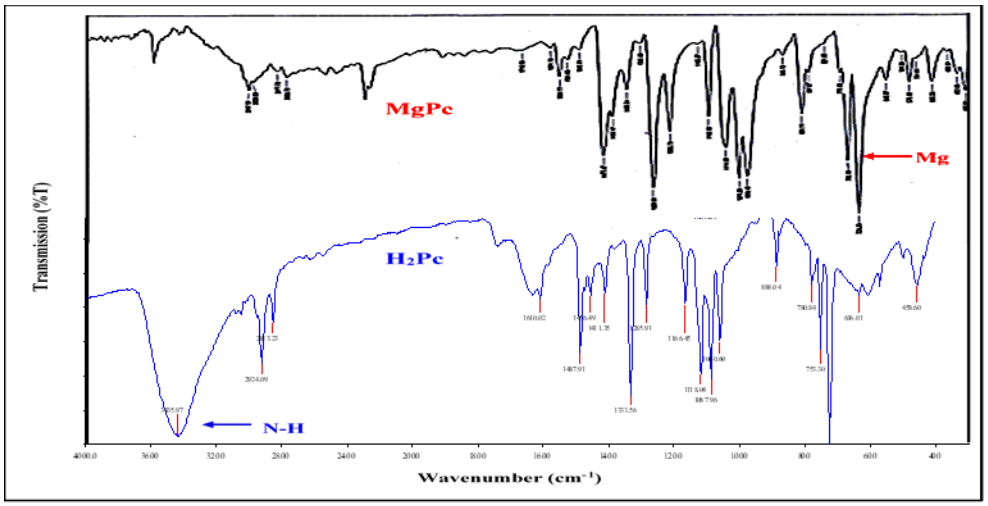

Figure 9: FTIR Spectra for MgPc and H_2Pc in the range (400 - 4000) cm^{-1}.

4. Conclusions

In this article, the structural properties of MgPc pure and thin films prepared by the Pulsed Laser Deposition (PLD) technique were investigated using FESEM, EDX, XRD, and AFM at different annealing temperatures (300, 373, 473, and 573) K. Various structural parameters, including grain size and surface roughness, were estimated, and it was observed that the morphological and structural properties improved with changes in temperature. It was concluded that as the annealing temperature increases, the material's crystallinity improves, enhancing the morphology of the thin film surfaces. It was demonstrated that annealing temperature plays an important role in the structure of deposited thin films. The recorded absorption spectra in the UV-Vis region displayed two absorption bands of the magnesium phthalocyanine (MgPc) molecule: the Soret (B-band) and the Q-band. The Q-band exhibited splitting characteristics (Davydov splitting). These absorption spectra were generally interpreted in terms of excitation. The impact of the annealing process on the absorption spectra of the studied films was examined. The absorption intensity was noted to increase slightly with the rising annealing temperature, ranging from 300 to 573 K.

Conflict of interest

Authors declare that they have no conflict of interest.

References

1. A. Kazak, M. Marchenkova, A. Smirnova, T. Dubinina, A. Seregin, A. Rogachev, and N. Usol'tseva, ITM Web Conf. **30**, 08006 (2019). DOI: 10.1051/itmconf/20193008006.
2. M. Pişkin, Ö. F. Öztürk, and Z. Odabaş, MANAS J. Eng. **9**, 58 (2021). DOI: 10.51354/mjen.884756.
3. S. Jain, R. Ridhi, N. Soleimanioun, S. Bharti, G. K. Bhullar, and S. K. Tripathi, AIP Conf. Proce. **2093**, 020041 (2019). DOI: 10.1063/1.5097110.
4. A. H. S. Mohammad and S. I. Mohammed, Kirkuk J. Sci. **15**, 45 (2020). DOI: 10.32894/kujss.2020.15.2.4.
5. G. D. Sharma, R. Kumar, and M. S. Roy, Sol. Ener. Mat. Sol. Cel. **90**, 32 (2006). DOI: 10.1016/j.solmat.2005.02.001.
6. M. S. Aziz, Sol. St. Elect. **50**, 1238 (2006). DOI: 10.1016/j.sse.2006.05.009.
7. S. Rajaputra, G. Sagi, and V. P. Singh, Sol. Ener. Mat. Sol. Cel. **93**, 60 (2009). DOI: 10.1016/j.solmat.2008.03.015.
8. Y. Ohmori, E. Itoh, and K. Miyairi, Thin Sol. Fil. **499**, 369 (2006). DOI: 10.1016/j.tsf.2005.07.027.
9. G. Ran, J. Wang, J. Yue, M. Pei, J. Chen, and W. Zhang, Chem. Phys. Lett. **751**, 137501 (2020). DOI: 10.1016/j.cplett.2020.137501.
10. C. Verma, E. E. Ebenso, M. A. Quraishi, and K. Y. Rhee, J. Molec. Liq. **334**, 116441 (2021). DOI: 10.1016/j.molliq.2021.116441.
11. J. F. Matoko-Ngouma, B. R. Malonda-Boungou, A. T. Raji, P. S. Moussounda, and B. M'passi-Mabiala, J. Molec. Struct. **1211**, 128034 (2020). DOI: 10.1016/j.molstruc.2020.128034.
12. G. Baburaya Kamath, C. M. Joseph, and C. S. Menon, Mat. Lett. **57**, 730 (2002). DOI: 10.1016/S0167-577X(02)00862-5.
13. N. J. Yutronkie, B. King, O. A. Melville, B. H. Lessard, and J. L. Brusso, J. Mater. Chem. C **9**, 10119 (2021). DOI: 10.1039/D1TC02275J.
14. N. Lanzetti, Y. Z. Lian, A. Cortinovis, L. Dominguez, M. Mercangöz, and C. Jones, 2019 18th European Control Conference (ECC) (Naples, Italy IEEE, 2019). p. 1005.
15. Y. Liu, X. Zhao, B. Cai, T. Pei, Y. Tong, Q. Tang, and Y. Liu, Nanoscale **6**, 1323 (2014). DOI: 10.1039/C3NR05680E.
16. M. F. Hasaneen, H. M. Ali, M. M. Abd El-Raheem, and A. M. Abdel Hakeem, Mat. Sci. Eng. B **262**, 114704 (2020). DOI: 10.1016/j.mseb.2020.114704.
17. M. Urbani, G. De La Torre, M. K. Nazeeruddin, and T. Torres, Chem. Soc. Rev. **48**, 2738 (2019). DOI: 10.1039/C9CS00059C.
18. S. N. Ogugua, O. M. Ntwaeaborwa, and H. C. Swart, Coatings **10**, 1078 (2020). DOI: 10.3390/coatings10111078.

19. E. Ortí, J. L. Brédas, and C. Clarisse, J. Chem. Phys. **92**, 1228 (1990). DOI: 10.1063/1.458131.
20. M. Abd El-Rahman, K. M. Yassien, and A. a. M. Yassene, Optik **183**, 962 (2019). DOI: 10.1016/j.ijleo.2018.12.182.
21. M. Socol, N. Preda, and G. Socol, Coatings **11**, 1368 (2021). DOI: 10.3390/coatings11111368.
22. K. R. Rajesh and C. S. Menon, Mat. Lett. **53**, 329 (2002). DOI: 10.1016/S0167-577X(01)00502-X.
23. E. Kavetsou, C. Tsoukalas-Koulas, A. Katopodi, A. Kalospyros, E. Alexandratou, and A. Detsi, Bioengineering **10**, 244 (2023). DOI: 10.3390/bioengineering10020244.
24. A. A. Ramadhan, Iraqi J. Phys. **15**, 131 (2019). DOI: 10.30723/ijp.v15i33.149.
25. E. K. Hassan, Iraqi J. Phys. **13**, 170 (2019). DOI: 10.30723/ijp.v13i28.255.
26. M. M. El-Nahass, A. A. Atta, H. E. A. El-Sayed, and E. F. M. El-Zaidia, Appl. Surf. Sci. **254**, 2458 (2008). DOI: 10.1016/j.apsusc.2007.09.064.
27. B. Olmos, C. Liedl, I. Lesanovsky, and P. Schneeweiss, Phys. Rev. A **104**, 043517 (2021). DOI: 10.1103/PhysRevA.104.043517.
28. A. M. Abdelghany, A. A. Menazea, and A. M. Ismail, J. Molec. Struct. **1197**, 603 (2019). DOI: 10.1016/j.molstruc.2019.07.089.
29. S. M. Khorsheed and N. M. Yaseen, J. Phys. Conf. Ser. **1897**, 012074 (2021). DOI: 10.1088/1742-6596/1897/1/012074.
30. A. Boguta, D. Wróbel, A. Bartczak, R. Swietlik, Z. Stachowiak, and R. M. Ion, Mat. Sci. Eng. B **113**, 99 (2004). DOI: 10.1016/j.mseb.2004.07.005.
31. P. Raji, C. Sanjeeviraja, and K. Ramachandran, Bull. Mater. Sci. **28**, 233 (2005). DOI: 10.1007/BF02711253.
32. R. E. Hummel, *Electronic Properties of Materials* (USA, Springer Science & Business Media, 2011).
33. R. Prabakaran, E. Fortunato, R. Martins, and I. Ferreira, J. Non-Crys. Sol. **354**, 2892 (2008). DOI: 10.1016/j.jnoncrysol.2007.10.096.
34. E. K. Hassan, NeuroQuantology **18**, 45 (2020). DOI: 10.14704/nq.2020.18.3.NQ20149.
35. N. S. Hamzah and E. K. Hassan, Int. J. Nanosci. **22**, 2350028 (2023). DOI: 10.1142/S0219581X2350028X.
36. R. Seoudi, G. S. El-Bahy, and Z. A. El Sayed, J. Molec. Struct. **753**, 119 (2005). DOI: 10.1016/j.molstruc.2005.06.003.

دراسة الخواص الفيزيائية لأغشية المغنسيوم فثالوسيانين (MgPc) الرقيقة بدرجات تلدين مختلفة محضرة بتقنية الترسيب بالليزر النبضي

نورا غسان عدنان[1] وإيمان كريم حسن[1]

[1]قسم الفيزياء، كلية العلوم، جامعة بغداد، بغداد، العراق

الخلاصة

تم ترسيب فثالوسيانين المغنيسيوم (MgPc) على ركيزة زجاجية بواسطة الترسيب بالليزر النبضي (PLD) باستخدام ليزر Nd:YAG Q-Switching بطول موجي 1064 نانومتر ومعدل تكرار 6 هرتز، في درجة حرارة الغرفة (300 كلفن) ودرجات حرارة التلدين المختلفة (373 و473 و573) كلفن تحت ظروف فراغ تبلغ 10^{-3} تور. تم تلدين جميع الأفلام لمدة ساعة واحدة لتحقيق التبلور. أشار حيود الأشعة السينية (XRD) لمسحوق MgPc إلى أن MgPc يتبلورفي متعدد البلورات مع بنية أحادية الميل. أثناء مقارنة أفلام MgPc لوحظ أن شدة الذروة المميزة تزداد مع درجة الحرارة، وأظهر التبلور بنية أحادية الميل نموذجية لشكل β. تم حساب قيم مؤشرات ميلر hkl لكل ذروة حيود في طيف XRD. تم العثور على الذروة المميزة للفثالوسيانين (MgPc) عند قيمة°6.9137 =2θ مع قيمة hkl (100) لكل من مسحوق MgPc والأغشية الرقيقة المترسبة. أشارت مجهر مسح الانبعاث الإلكتروني الميداني (FE-SEM) وتحليلات مطيافية الأشعة السينية المشتتة للطاقة (EDX) والمجهر الذري للقوة (AFM) إلى تحسن التبلور وتعزيز مورفولوجيا السطح مع ارتفاع درجة حرارة التلدين وأظهرت حبيبات ذات أحجام موحدة. كما ساعدوا في تحديد المعلمات المثلى التي أسفرت عن أفضل الخصائص البنيوية للغشاء. أظهرت الخصائص البصرية للأغشية الرقيقة MgPc نطاقي امتصاص. تُظهر الأغشية الرقيقة MgPc فجوات طاقة مباشرة للنقل والبداية (E_g) لجميع العينات. بالإضافة إلى ذلك، تم حساب معامل الامتصاص (α) باستخدام قانون لامبرت، مما يكشف عن اعتماد طفيف على درجة حرارة التلدين. تم تحديد أطياف FT-IR لـ (MgPc) و (H_2Pc).

الكلمات المفتاحية: مغنيسيوم فثالوسيانين العضوي، تقنية الترسيب بالليزر النبضي، تقنية مجهر مسح إلكتروني بالانبعاث الميداني، تقنية مجهر القوة الذرية، فجوة الطاقة.